COMPUTATIONAL SIMULATION OF PROBABILISTIC LIFETIME STRENGTH FOR AEROSPACE MATERIALS SUBJECTED TO HIGH TEMPERATURE, MECHANICAL FATIGUE, CREEP AND THERMAL FATIGUE

Prepared by:

Lola Boyce, Ph. D., P. E., Principal Investigator
Callie C. Bast, B.S.M.E., Graduate Research Assistant
Greg A.Trimble, Undergraduate Research Assistant

Final Technical Report
of Project Entitled
Development of Advanced Methodologies
for Probabilistic Constitutive Relationships
of Material Strength Models, Phase 4

NASA Grant No. NAG 3-867, Supp. 4

Report Period:
January 1991 to August 1992

Prepared for:

NATIONAL AERONAUTICS AND SPACE ADMINISTRATION
Lewis Research Center
Cleveland, Ohio 44135

The Division of Engineering
The University of Texas at San Antonio
San Antonio, TX 78249
August, 1992

TABLE OF CONTENTS

PREFACE

The University of Texas at San Antonio (UTSA) is a relatively new university. It was established in 1969 and opened for classes in 1973. As the only comprehensive public university serving the nation's ninth largest city, it was and is vital to San Antonio and the entire South Texas Region. In 1982, ten years ago, an undergraduate engineering program was established at UTSA with the support of the community and its leaders. Today, all three undergraduate engineering programs are ABET accredited and serve about 1000 students, a significant percentage of whom are Hispanic. A new engineering building, containing laboratory facilities and equipment, opened in January, 1991. Furthermore, a graduate program has just been put in place at the M.S. level and one is planned at the Ph.D. level. The first Master's Degree students enrolled in Fall, 1989.

Naturally, the engineering research environment is just developing at UTSA. Now, thanks in great measure to the UT System support and this ongoing NASA grant, good progress is being made. Specifically, the purchase of a UT System Cray-Y-MP in November, 1990 has provided a world-class analytical and numerical research environment not ordinarily available to a new university. As a result the UTSA Supercomputer Network Research Facility (SNRF) was developed by the principal investigator, Dr. Lola Boyce. This has allowed the successful completion of this research project, an early one of its kind at UTSA.

This NASA research grant has allowed three undergraduate engineering students, Eddie Aponte, Greg Trimble and Paul Van Veen, plus the first UTSA Mechanical Engineering graduate student, Callie Bast, to work directly with the principal investigator, Dr. Boyce, providing them with a quality research experience they would otherwise probably not have had. All undergraduate students have expressed an interest in continuing their education at the graduate level.

In conclusion, and in view of the significant accomplishments in fundamental research, enhancement of the engineering research environment at UTSA, and direct support of Mechanical Engineering students, it is hoped that the proposed extension of this grant will receive favorable consideration at NASA. The principal investigator sincerely thanks NASA for funding this fourth year grant.

ABSTRACT

This report presents the results of a fourth year effort of a research program conducted for NASA-LeRC by The University of Texas at San Antonio (UTSA). The research included on-going development of methodology that provides probabilistic lifetime strength of aerospace materials via computational simulation. A probabilistic material strength degradation model, in the form of a randomized multifactor interaction equation, is postulated for strength degradation of structural components of aerospace propulsion systems subjected to a number of effects or primitive variables. These primitive variables may include high temperature, fatigue or creep. In most cases, strength is reduced as a result of the action of a variable. This multifactor interaction strength degradation equation has been randomized and is included in the computer program, PROMISS. Also included in the research is the development of methodology to calibrate the above-described constitutive equation using actual experimental materials data together with regression analysis of that data, thereby predicting values for the empirical material constants for each effect or primitive variable. This regression methodology is included in the computer program, PROMISC. Actual experimental materials data were obtained from industry and the open literature for materials typically for applications in aerospace propulsion system components. Material data for Inconel 718 has been analyzed using the developed methodology.

LIST OF FIGURES

LIST OF FIGURES

LIST OF TABLES

1.0 INTRODUCTION

This report presents the results of a fourth year effort of a research program entitled "Development of Advanced Methodologies for Probabilistic Constitutive Relationships of Material Strength Models, Phase 4." This research is sponsored by the National Aeronautics and Space Administration-Lewis Research Center (NASA-LeRC). The principal investigator is Dr. Lola Boyce, Associate Professor of Mechanical Engineering, The University of Texas at San Antonio (UTSA). The objective of the research program is the development of methodology that provides probabilistic lifetime strength of aerospace materials via computational simulation.

As part of this fourth year effort, a material strength degradation model, in the form of a randomized multifactor interaction equation, is postulated for strength degradation of structural components of aerospace propulsion systems subjected to a number of effects or primitive variables. These primitive variables often originate in the environment and may include high temperature, fatigue and creep. In most cases, strength is reduced as a result. Also included in the research is the development of methodology to calibrate the multifactor interaction equation using actual experimental materials data together with a regression analysis of that data, thereby predicting values for the empirical material constants for each effect or primitive variable. Material data for Inconel 718 has been analyzed using the developed methodology. Sections 2.0 and 3.0 summarize the theoretical and computational background for the research.

The above-described randomized multifactor interaction equation is included in the computer program, PROMISS. Calibration of the equation by multiple regression analysis of the data may be carried out using the statistical regression computer program, PROMISC. These programs were developed using the UTSA Supercomputer Network Research Facility (SNRF) Cray Y-MP. The latest versions (Ver. 2.0) of these programs are obtainable from the principal investigator at the address given on the cover page of this report.

Sections 4.0 through 7.0 address specific tasks described in the proposal for this research "Development of Advanced Methodologies for Probabilistic Constitutive Relationships for Material Strength Models, Phase 4", 1991. Specifically, Section 4.0 discusses the strength degradation model developed for the high temperature, mechanical fatigue and creep effects of Inconel 718. Section 5.0 introduces the thermal fatigue strength degradation model, a new effect included in the multifactor interaction equation. Section 6.0 presents experimental material data for Inconel 718 and displays the data in the form utilized in the multifactor interaction equation model. High temperature, mechanical fatigue, creep and thermal fatigue data are displayed. This data may be used in the development of data for the PROMISS resident database. Section 7.0 presents and discusses cases for analysis that resulted from a sensitivity study, utilizing the PROMISS "flexible" capability. The cases show the effect on probabilistic lifetime strength for several effects, including high temperature, mechanical fatigue and creep. This sensitivity study is the first such study to begin to account for synergistic effects.

A paper was produced documenting much of the effort of this fourth year research program. It is entitled "Computational Simulation of Coupled Material Degradation Processes for Probabilistic Lifetime Strength of Aerospace Materials", by L. Boyce and C. C. Chamis. It was presented at the AIAA/SAE/ASME/ASEE Joint Propulsion Conference, Nashville, TN, July, 1992 and is published in the Proceedings. It has also been submitted to the ASME Journal of Engineering for Gas Turbines and Power and a copy is included with this report.

2.0 THEORETICAL BACKGROUND

Recently, a general material strength degradation model, for composite materials subjected to a number of diverse effects or primitive variables, has been postulated to predict mechanical and thermal material properties [1, 2, 3, 4]. The resulting multifactor interaction constitutive equation summarizes composite micromechanics theory and has been used to predict material properties for a unidirectional fiber-reinforced lamina, based on the corresponding properties of the constituent materials.

These equations have been modified to predict the lifetime strength for a single constituent material due to "n" diverse effects or variables [5, 6, 7]. These effects could include variables such as high temperature, creep, mechanical fatigue, thermal fatigue, corrosion, strain rate effects, and so forth. For most of these variables, strength has been observed to decrease with an increase in the variable. This report presents the results of work to use the modified multifactor interaction equation to account for the degradation of lifetime strength due to three variables, high temperature, mechanical fatigue and creep. The report also presents an extension of the model to account for thermal fatigue effects. The general form of the postulated multifactor interaction equation is

$$\frac{S}{S_O} = \prod_{i=1}^{n} \left[\frac{A_{iU} - A_i}{A_{iU} - A_{iO}}\right]^{a_i}, \qquad (1)$$

where A_i, A_{iU} and A_{iO} are the current, ultimate and reference values, respectively, of a particular effect; a_i is the value of an empirical constant for the i^{th} product term in the model; S and S_O are the current and reference values of material strength and n is the number of product terms in the model. Each term has the property that if the current value equals the ultimate value, the current strength will be zero. Also, if the current value equals the reference value, the term equals one and strength is not affected by that variable.

This deterministic material strength degradation model may be calibrated by an appropriately curve-fitted least squares linear regression of experimental data [8], perhaps supplemented by expert opinion. Ideally, experimental data giving the relationship between effects and strength is obtained. For example, data for just one effect could be plotted on log-log paper. A good fit for the data may then be obtained by a linear regression analysis. This is illustrated schematically in Figure 1. The equation, for a single effect, is then obtained by noting the linear relation between log S and log $[(A_U - A_O)/(A_U - A)]$, as follows:

$$\log S = - a \log\left[\frac{A_U - A_O}{A_U - A}\right] + \log S_O$$

$$\log S - \log S_O = - a \log\left[\frac{A_U - A_O}{A_U - A}\right]$$

$$\log \frac{S}{S_O} = - a \log\left[\frac{A_U - A_O}{A_U - A}\right]$$

$$\frac{S}{S_O} = \left[\frac{A_U - A_O}{A_U - A}\right]^{-a} \qquad (2a)$$

$$\frac{S}{S_O} = \left[\frac{A_U - A}{A_U - A_O}\right]^a \qquad (2b)$$

Equation (2a) is for a variable that lowers strength. Notice that if a variable raises strength the exponent, a, in equation (2a) is negative.

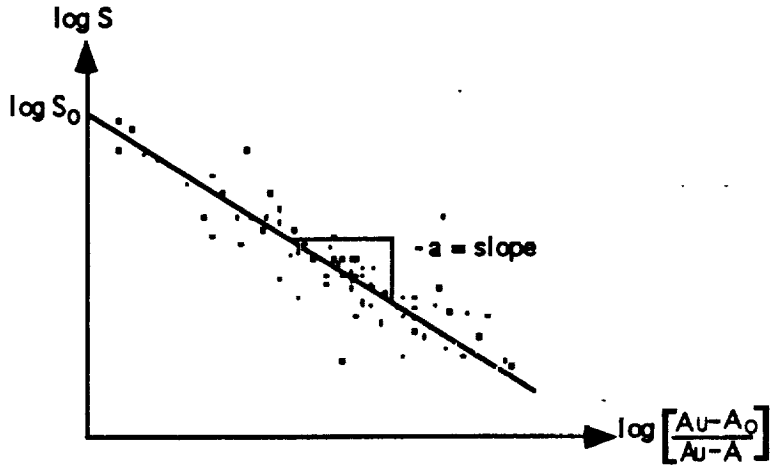

Fig. 1 Schematic of Data Illustrating the Effect of One Primitive Variable on Strength.

This general material strength degradation model, given by equation (1) may be used to estimate the lifetime strength, S/S_O, of an aerospace propulsion system component under the influence of a number of diverse effects or primitive variables. The probabilistic treatment of this model includes randomizing the deterministic multifactor interaction equation, performing probabilistic analysis by simulation and generating probability density function (p.d.f.) estimates for strength using the non-parametric method, maximum penalized likelihood [9, 10]. Integration of the probability density function yields the cumulative distribution function (c.d.f.) from which probability statements regarding strength may be made. This probabilistic material strength degradation model predicts the random strength of an aerospace propulsion system component subjected to a number of diverse random effects.

The probabilistic constitutive model is embodied in two FORTRAN programs, PROMISS (Probabilistic Material Strength Simulator) and PROMISC (Probabilistic Material Strength Calibrator)[6]. PROMISS calculates the random strength of an aerospace propulsion component due to as many as eighteen diverse random effects. Results are presented in the form of probability density functions and cumulative distribution functions of lifetime strength, S/S_O. PROMISC calculates the values of the empirical material constants, a_i.

3.0 PROMISS AND PROMISC COMPUTER PROGRAMS

PROMISS includes a relatively simple "fixed" model as well as a "flexible" model. The fixed model postulates a probabilistic multifactor interaction equation that considers the variables given in Table 1 (see p. 5). The general form of this constitutive equation is given in equation (1), wherein there are now n = 7 product terms, one for each effect or primitive variable listed above. Note that since this model has seven variables, each containing four values of the variable, it has a total of twenty-eight variables. The flexible model postulates the probabilistic multifactor interaction equation that considers up to as many as n = 18 product terms for primitive variables. These variables may be selected to utilize the theory and experimental data currently available for the specific strength degradation mechanisms of interest. The specific effects included in the flexible model are listed in Table 2. Note that in order to provide for future expansion and customization of the flexible model, six "other" effects have been provided.

Table 2 Variables Available in the "Flexible" Model.

A. Environmental Effects

1. Mechanical
   a. Stress
   b. Impact
   c. Other Mechanical Effect
2. Thermal
   a. Temperature Variation
   b. Thermal Shock
   c. Other Thermal Effect
3. Other Environmental Effects
   a. Chemical Reaction
   b. Radiation Attack
   c. Other Environmental Effect

B. Time-Dependent Effects

1. Mechanical
   a. Creep
   b. Mechanical Fatigue
   c. Other Mech. Time-Dependent. Effect
2. Thermal
   a. Thermal Aging
   b. Thermal Fatigue
   c. Other Thermal Time-Dependent. Effect
3. Other Time-Dependent Effects
   a. Corrosion
   b. Seasonal Attack
   c. Other Time-Dependent. Effect

Table 1 Variables Available in the "Fixed" Model.

i^{th} Primitive Variable	Primitive Variable Type
1	Stress due to static load
2	Temperature
3	Chemical reaction
4	Stress due to impact
5	Mechanical fatigue
6	Thermal fatigue
7	Creep

The considerable scatter of experimental data and the lack of an exact description of the underlying physical processes for the combined mechanisms of fatigue, creep, temperature variations, and so on, make it natural, if not necessary to consider probabilistic models for a strength degradation model. Therefore, the fixed and flexible models corresponding to equation (1) are "randomized", and yield the "random lifetime material strength due to a number of diverse random effects." Note that for the fixed model, equation (1) has the following form:

$$S/S_O = f(A_{1U}, A_1, A_{1O}, a_1,..., A_{iU}, A_i, A_{iO}, a_i,..., A_{7U}, A_7, A_{7O}, a_7) \quad (3)$$

where A_i, A_{iU} and A_{iO} are the current, ultimate and reference values of the i^{th} of seven effects or primitive variables as given in Table 1, and a_i is the ith empirical material constant. In general, this expression can be written as,

$$S/S_O = f(X_i),\ i = 1,..., 28, \quad (4)$$

where the X_i are the twenty eight independent variables in equation (3). Thus, the fixed model is "randomized" by assuming all the independent variables, X_i, i = 1,..., 28, to be random and stochastically independent. For the flexible model, equation (1) has a form analogous to equations (3) and (4), except that there are as many as seventy-two independent variables. Applying probabilistic analysis to either of these randomized equations yields the distribution of the dependent random variable, lifetime material strength, S/S_O.

Although a number of methods of probabilistic analysis are available[9], simulation was chosen for PROMISS. Simulation utilizes a theoretical sample generated by numerical techniques for each of the independent random variables. One value from each sample is substituted into the functional relationship, equation (3), and one realization of lifetime strength, S/S_O, is calculated. This calculation is repeated for each value in the set of samples, yielding a distribution of different values for lifetime strength.

A probability density function is generated from these different values of lifetime strength, using a non-parametric method, maximum penalized likelihood. Maximum penalized likelihood generates the p.d.f. estimate using the method of maximum likelihood together with a penalty function to smooth it [10]. Finally, integration of the generated p.d.f. results in the cumulative distribution function, from which probabilities of lifetime strength can be directly observed.

In summary, PROMISS randomizes the following equation:

$$\frac{S}{S_O} = \prod_{i=1}^{n} \left[\frac{A_{iU} - A_i}{A_{iU} - A_{iO}}\right]^{a_i}, \tag{1}$$

where

$$\left[\frac{A_{iU} - A_i}{A_{iU} - A_{iO}}\right]^{a_i}$$

is the i^{th} effect; A_i, A_{iU} and A_{iO} are random variables; a_i is the i^{th} empirical material constant and S/S_O is lifetime strength. There is a maximum of eighteen possible effects or primitive variables that may be included in the model. For the flexible model option, they may be chosen by the user from those in Table 2. For the fixed model option, the variables of Table 1 are used. Within each primitive variable term, the current, ultimate and reference values as well as the empirical material constant, may be modeled as either deterministic (i.e., empirical, calculated by PROMISC), normal, lognormal, or Wiebull random variables. Simulation is used to generate a set of realizations for lifetime random strength, S/S_O, from a set of realizations for primitive variables and empirical material constants. Maximum penalized likelihood is used to generate an estimate for the p.d.f. of lifetime strength, from a set of realizations of lifetime strength. Integration of the p.d.f. yields the c.d.f. Plot files are produced to plot both the p.d.f. and the c.d.f. PROMISS also provides information on lifetime strength, S/S_O, statistics (mean, variance, standard deviation and coefficient of variation). A resident database is included in PROMISS and may be used to provide user input for the empirical material constants.

PROMISC performs a multiple linear regression on actual experimental or simulated experimental data for as many as eighteen effects or primitive variables, yielding regression coefficients that are the empirical material constants, a_i, required by PROMISS. It produces the linear regression of the log transformation of equation (1), the multifactor interaction equation. When transformed it becomes

$$\log \frac{S}{S_O} = \sum_{i=1}^{18} -a_i \log\left[\frac{A_{iU} - A_{iO}}{A_{iU} - A_i}\right] \tag{5}$$

or

$$\log S = \log S_O + \sum_{i=1}^{18} -a_i \log\left[\frac{A_{iU} - A_{iO}}{A_{iU} - A_i}\right], \tag{6}$$

where

$$\left[\frac{A_{iU} - A_{iO}}{A_{iU} - A_i}\right]^{-a_i}$$

is the i^{th} effect, A_i, A_{iU} and A_{iO} are primitive variable data and a_i is the i^{th} empirical material constant, or the i^{th} regression coefficient to be predicted by PROMISC. Also, log S_O is the log transformed reference value of strength, or the intercept regression coefficient to be predicted by PROMISC, and log S is the log transformed current value of strength. Experimental data for up to eighteen possible effects, as given in Table 2, may be included. The variable data may be either actual experimental data or expert opinion, directly read from input, or simulated data where expert opinion is specified as the mean and standard deviation of a normal or lognormal distribution. The simulated data option for input data was used in the early stages of code development to verify correct performance. The input data, whether actual or simulated, is read in and assembled into a data matrix. From this data matrix, a corrected sums of squares and cross products matrix is computed. From this sums of squares and cross products matrix, and a least squares methodology, a multiple linear regression is performed to calculate estimates for the empirical material constant, a_i, and the reference strength, S_O. These are the regression coefficients.

PROMISC includes enhancements of the multiple linear regression analysis to screen data from "outliers" and collinearities; to determine "how well" the data fit the regression; to quantify the importance and relative importance of each factor in the multifactor interaction equation (1), as well as, to check assumptions inherent in the use of multiple linear regression. Further details are provided in Reference 6, Section 6.0.

4.0 STRENGTH DEGRADATION MODELS FOR HIGH TEMPERATURE, MECHANICAL FATIGUE AND CREEP FOR INCONEL 718

The multifactor interaction equation for material strength degradation, given by equation (1), when modified for high temperature, fatigue and creep becomes,

$$\frac{S}{S_O} = \left[\frac{T_M - T_O}{T_M - T}\right]^{-q} \left[\frac{N_U - N_O}{N_U - N}\right]^{-s} \left[\frac{t_U - t_O}{t_U - t}\right]^{-v}, \tag{7}$$

where T_M is the ultimate or melting temperature of the material, T_O is a reference or room temperature, T is the current temperature, N_U is the ultimate number of cycles (for which fatigue strength is very small), N_O is a reference number of cycles (for which fatigue strength is very large), N is the current number of cycles the material has undergone, t_U is the ultimate number of creep hours (for which rupture strength is very small), t_O is a reference number of creep hours (for which rupture strength is very large) and t is the current number of creep hours. Also q, s and v are empirical material parameters, one for each variable, that represent the slope of a straight line fit of the data on log-log paper.

The appropriate values for ultimate and reference quantities must be selected prior to calibration of the multifactor interaction equation for Inconel 718. For example, for Inconel 718 the melting temperature is $T_M = 2369$ °F. Hence equation (7), for Inconel 718, becomes

$$\frac{S}{S_O} = \left[\frac{2369 - 75}{2369 - T}\right]^{-q} \left[\frac{10^{10} - 0.5}{10^{10} - N}\right]^{-s} \left[\frac{10^6 - 1.0}{10^6 - t}\right]^{-v}. \tag{8}$$

The ultimate and reference quantities given in equation (8) become model parameters or constraints for the multifactor interaction equation when modified for Inconel 718. Figure 2 illustrates these model parameters graphically wherein each axis represents an effect or primitive variable. Note also an additional constraint in Figure 2, namely the creep threshold temperature, $T_C = 900$ °F. Although this constraint is not explicitly built into the multifactor interaction equation, it may be taken into account indirectly. This is accomplished by not including the creep effect whenever the current value of temperature, T, is below 900 °F. Note that the empirical material parameters, q, s and v must be determined from actual experimental data.

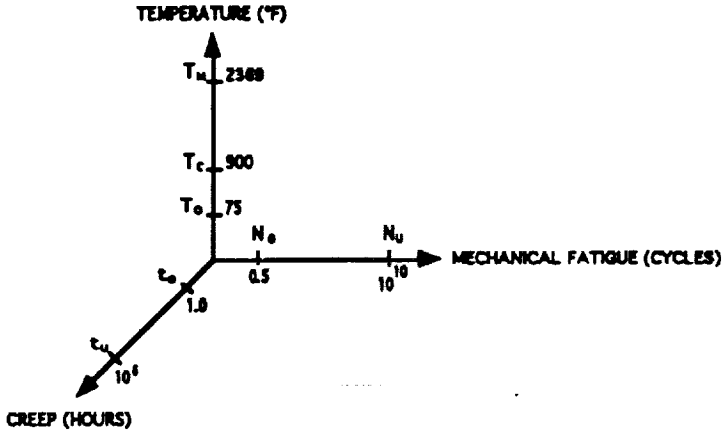

Fig. 2 Model Parameters for Inconel 718 for Temperature, Mechanical Fatigue and Creep.

5.0 STRENGTH DEGRADATION MODEL FOR THERMAL FATIGUE

The general model for the thermal fatigue effect uses stress-life (σ-N) data obtained from experimental strain-life (ε-N) data. Total strain amplitude data [14] and plastic strain amplitude data [12] were used to construct a strain-life curve. The plastic portion of the curve may be represented by the following power law function:

$$\frac{\Delta\varepsilon_P}{2} = \varepsilon_F' (2N_F)^c , \tag{9}$$

where $\Delta\varepsilon_P/2$ is the plastic strain amplitude, $2N_F$ is the reversals to failure. A power law regression analysis of the data yields two thermal fatigue properties, namely, the fatigue ductility coefficient, ε_F', and the fatigue ductility exponent, c. Regression statistics, such as the coefficient of determination, R^2, may show that a power law representation of the relationship between plastic strain amplitude and reversals to failure is satisfactory.

Stress amplitude, $\Delta\sigma/2$, can be calculated using the modulus of elasticity, E, and the total and plastic strain amplitudes, $\Delta\varepsilon_T/2$ and $\Delta\varepsilon_P/2$ respectively, from

$$\frac{\Delta\sigma}{2} = E\left[\frac{\Delta\varepsilon_T}{2} - \frac{\Delta\varepsilon_P}{2}\right]. \tag{10}$$

When the resulting stress amplitude is plotted against plastic strain amplitude the cyclic stress-strain plot results. Again, a power law function may be satisfactory for expressing the cyclic stress-strain relationship. The function is

$$\frac{\Delta\sigma}{2} = K'\left(\frac{\Delta\varepsilon_P}{2}\right)^{n'}, \tag{11}$$

where K' is the cyclic strength coefficient and n' is the cyclic strain hardening exponent, two additional thermal fatigue properties.

When the stress amplitude is plotted against reversals to failure, the stress-life plot results. A power law function may represent a good fit to the data. This function is

$$\frac{\Delta\sigma}{2} = \sigma'_F (2N_F)^b \tag{12}$$

where σ'_F is the fatigue strength coefficient and b is the fatigue strength exponent. These final two properties complete the set of thermal fatigue material properties.

With the ordinate now expressed in stress units (psi), a fourth effect can be added to the multifactor interaction model depicted by equations (7) and (8). This effect will have the form,

$$\left[\frac{N'_U - N'_O}{N'_U - N'}\right]^{-u} = \left[\frac{10^5 - 0.5}{10^5 - N}\right]^{-u},$$

where $N'_U = 10^5$ is the ultimate number of thermal cycles (for which thermal fatigue strength is very small), $N'_O = 0.5$ is the selected reference number of thermal cycles (for

which thermal fatigue strength is very large), N' is the current number of thermal cycles the material has undergone and u is an empirical material constant found from a power law regression of the data. Thus, equations (7) and (8) will have four terms, one for each effect,

$$\frac{S}{S_O} = \left[\frac{T_M - T_O}{T_M - T}\right]^{-q} \left[\frac{N_U - N_O}{N_U - N}\right]^{-s} \left[\frac{t_U - t_O}{t_U - t}\right]^{-v} \left[\frac{N'_U - N'_O}{N'_U - N'}\right]^{-u}, \tag{13}$$

$$\frac{S}{S_O} = \left[\frac{2369 - 75}{2369 - T}\right]^{-q} \left[\frac{10^{10} - 0.5}{10^{10} - N}\right]^{-s} \left[\frac{10^6 - 1.0}{10^6 - t}\right]^{-v} \left[\frac{10^5 - 0.5}{10^5 - N'}\right]^{-u}, \tag{14}$$

6.0 EXPERIMENTAL MATERIAL DATA FOR INCONEL 718

The multifactor interaction equation, specific for Inconel 718, requires the collection of experimental data to determine the empirical material constants, a_i. A computerized literature search of Inconel 718, a nickel-base superalloy, was conducted to obtain existing experimental data on various material properties. Data on high temperature tensile strength, mechanical fatigue strength and creep rupture strength properties were obtained for Inconel 718 [14, 15, 16, 17].

Inconel 718 data for high-temperature tensile strength, mechanical fatigue strength and creep rupture strength resulted from tests done on various hot and cold worked specimens [14,16]. Tests were conducted on sheets of Inconel 718 and hot rolled bars of the superalloy.

Low cycle fatigue produces cumulative material damage and ultimate failure in a component by the cyclic application of strains that extend into the plastic range. Failure typically occurs under 10^5 cycles. Low cycle fatigue is often produced mechanically, at a given temperature. It is even more common to observe a machine part that undergoes low cycle fatigue, producing cyclic strains due to a cyclic thermal field. These cyclic temperature changes produce thermal expansions and contractions that, if constrained, produce cyclic strains and stresses. These thermally induced stresses and strains will result in fatigue failure just as those produced by external mechanical loading produce fatigue failure.

Low cycle fatigue tests, comparing both mechanically strain cycled specimens at constant elevated temperatures and thermally cycled constrained specimens, have been conducted on stainless steel [11] and Inconel [12]. Results are typically plotted as plastic strain range versus cycles to failure. For stainless steel, these plots show that for equal values of plastic strain range the number of cycles to failure was much *less* for the thermally cycled specimens than for the mechanically cycled ones. To bring the thermal fatigue test results into coincidence with the isothermal mechanical fatigue test results [13], requires the multiplication of the strain, for any number of cycles to failure, by a factor of approximately 2.5. Inconel, however, responds to mechanically produced plastic strain in the *same* manner as it responds to thermally produced plastic strain. Thus, the Inconel test results provide a means for utilizing mechanically cycled data to build a thermal fatigue model for Inconel 718.

Inconel plastic strain data used for thermal fatigue was obtained by thermal excursions about a mean temperature of 1300 °F [12]. Since Inconel responds to mechanically produced plastic strain in the same manner as it responds to thermally produced plastic strain, total strain data obtained from mechanically produced strain tests was used for the thermal fatigue model [14]. These data are given in Table 3 and displayed as the strain life curves shown in Figure 3. Using data for the modulus of elasticity for Inconel 718 at 1300 °F, namely, $E = 23 \times 10^6$ psi [14], the stress amplitude can be calculated from equation (10). Hence, stress amplitude is plotted against plastic strain amplitude to produce the cyclic stress-strain curve shown in Figure 4. Using the power law regression techniques [18] indicated in equations (9), (11), and (12), and the data from Table 4, the thermal fatigue material properties for Inconel 718 can be calculated. These material properties are displayed in Table 5 and indicated graphically, along with their coefficient of determination, R^2, in Figures 5, 6, and 7. Although the values calculated for the exponents, b, c, n', are close to the range for most metals, the values of the

coefficients, K' and σ'_F are extremely high. These high values may be due in part to the following reasons:

(1) The thermal fatigue plastic strain data [12] was obtained from tests conducted on Inconel rather than Inconel 718.

(2) The total strain data [14] used for the thermal fatigue model was obtained from mechanical fatigue tests conducted at room temperature rather than at a temperature of 1300 °F, which was the mean temperature used for the thermal fatigue tests.

(3) The direct correlation found between the mechanical strain-cycled results under isothermal conditions and those obtained by thermally-cycling about a corresponding mean temperature was for the plastic strain and not the total strain component.

The Inconel 718 data selected was plotted in various forms, one of which was the same as that used by the multifactor interaction equation in PROMISS and PROMISC. The data plotted in Figures 8 and 9 show the effect of temperature on yield strength for Inconel 718. Figure 8 is the raw data and Figure 9 shows the data in the same form as that used in the multifactor interaction equation. As expected, the yield strength of the material decreases as the temperature increases. Figures 10 and 11 display data for the effect of mechanical fatigue cycles on fatigue strength for Inconel 718 for a given test temperature. As expected, the fatigue strength of the material decreases as the number of cycles increases. Figures 12 and 13 show data for the effect of creep time on rupture strength for Inconel 718 for a given temperature. As expected, the rupture strength of the material decreases as the time increases. Figures 14 and 15 display data for the effect of thermal fatigue cycles on stress amplitude at failure (i.e., thermal fatigue strength) for Inconel 718 for a mean thermal cycling temperature of 1300 °F. As expected, the thermal fatigue strength of the material decreases as the number of cycles increases.

A linear regression of the data for temperature, mechanical fatigue, creep and thermal fatigue, produces a first estimate of the empirical material constants for these effects, namely, q, s, v and u. Figures 16, 17, 18, and 19 show the results of linear regression and indicate values for the four material constants.

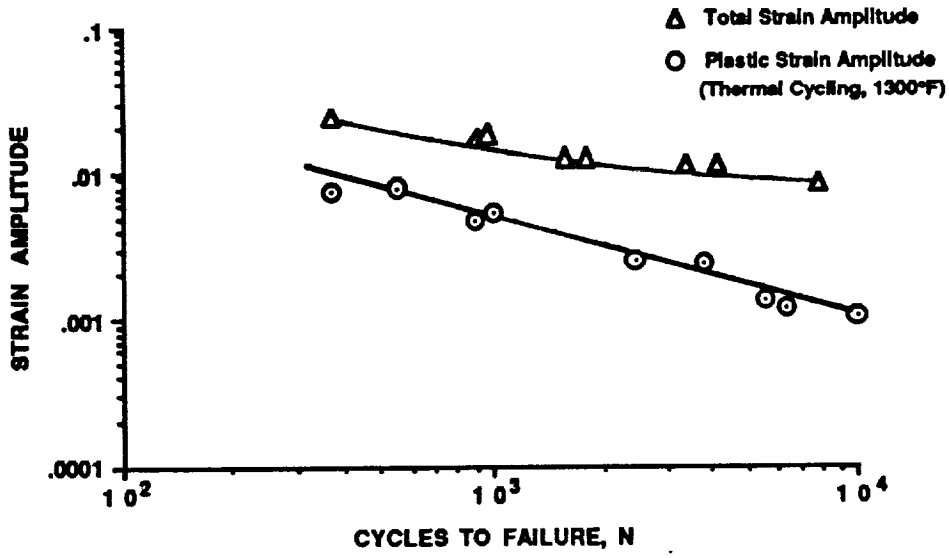

Fig. 3 Strain - life Curve for INCONEL 718

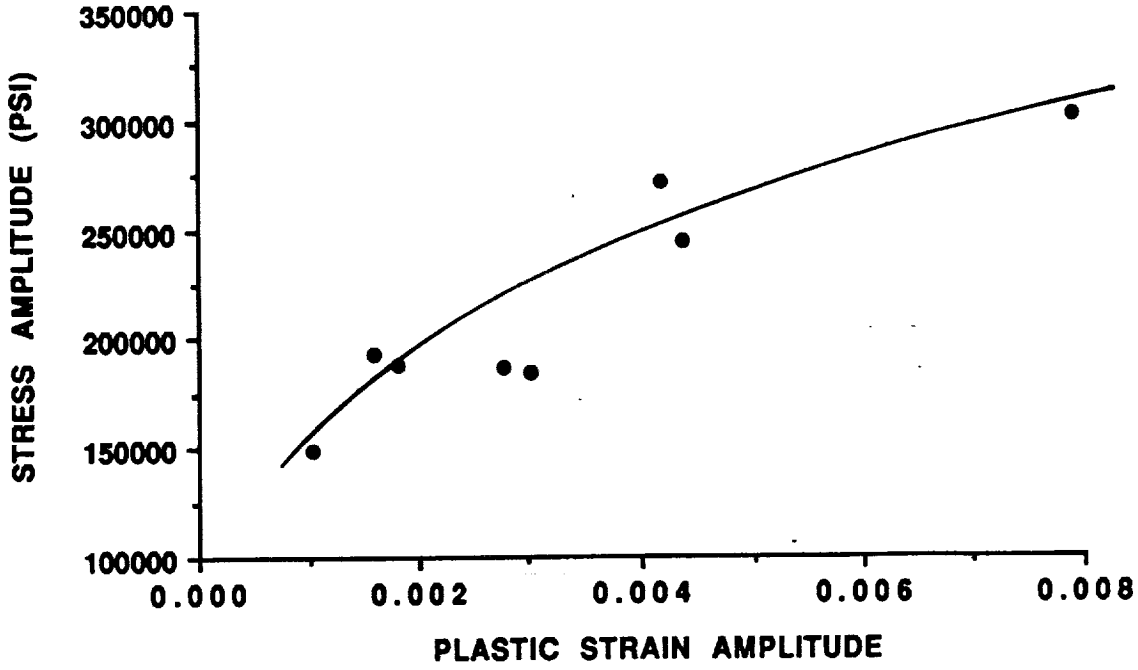

Fig. 4 Cyclic Stress-strain Curve for Inconel 718

Table 3 Thermal Fatigue Data for Inconel 718

Cycles to Failure N_F	Total Strain Amplitude, $\Delta\varepsilon_T/2$	Plastic Strain Amplitude, $\Delta\varepsilon_P/2$
350	0.021	0.007
520		0.007
840		0.004
850	0.015	
910	0.016	
950		0.005
1500	0.011	
1700	0.011	
2300		0.002
3200	0.010	
3600		0.002
3900	0.010	
5300		0.001
6000		0.001
7400	0.007	
9300		0.001

Table 4 Thermal Fatigue Data Reduced for Thermal Fatigue Material Properties

Reversals to Failure $2N_F$	Total Strain Amplitude, $\Delta\varepsilon_T/2$	Plastic Strain Amplitude, $\Delta\varepsilon_P/2$	Stress Amplitude, $\Delta\sigma/2$
700	0.021	0.0079	302,012
1700	0.015	0.0044	244,437
1820	0.016	0.0042	271,878
3000	0.011	0.0030	183,964
3400	0.0109	0.0028	187,156
6400	0.01	0.0018	188,203
7800	0.01	0.0016	193,336
14800	0.0075	0.0010	148,511

*These values use plastic strain amplitude regression line values.

Table 5 Thermal Fatigue Material Properties for Inconel 718

Fatigue Ductility Coefficient, ε'_F	0.6028
Fatigue Ductilty Exponent, c	-0.66228
Cyclic Strength Coefficient, K'	1.505×10^6 psi
Cyclic Strain Hardening Exponent, n'	0.33492
Fatigue Strength Coefficient, σ'_F	1.270×10^6 psi
Fatigue Strength Exponent, b	-0.2218

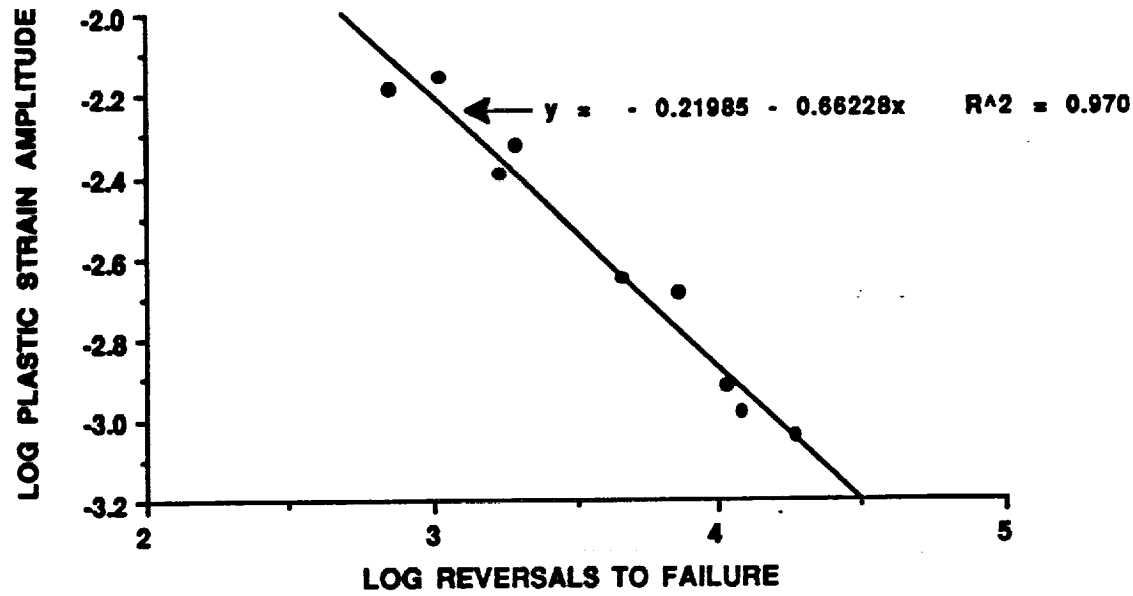

Fig. 5 Regression of Equation (9) Data Yielding Fatigue Ductility Coefficient, ε'_F, and Fatigue Ductility Exponent, c.

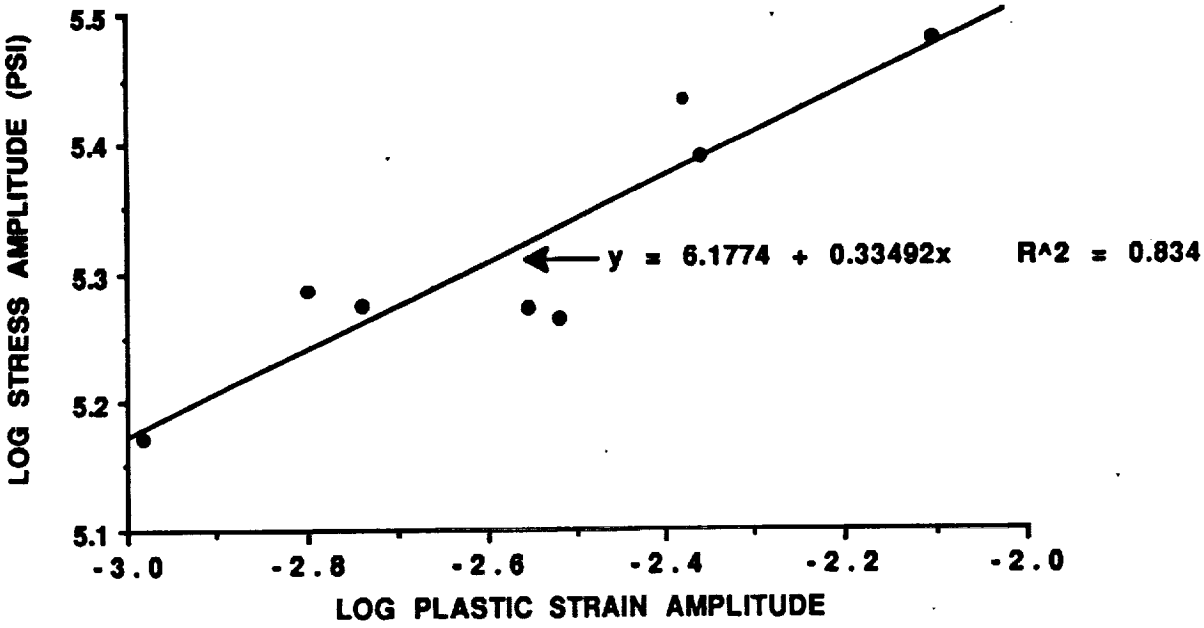

Fig. 6 Regression of Equation (11) Data Yielding Cyclic Strength Coefficient, K', and Cyclic Strain Hardening Exponent, n'.

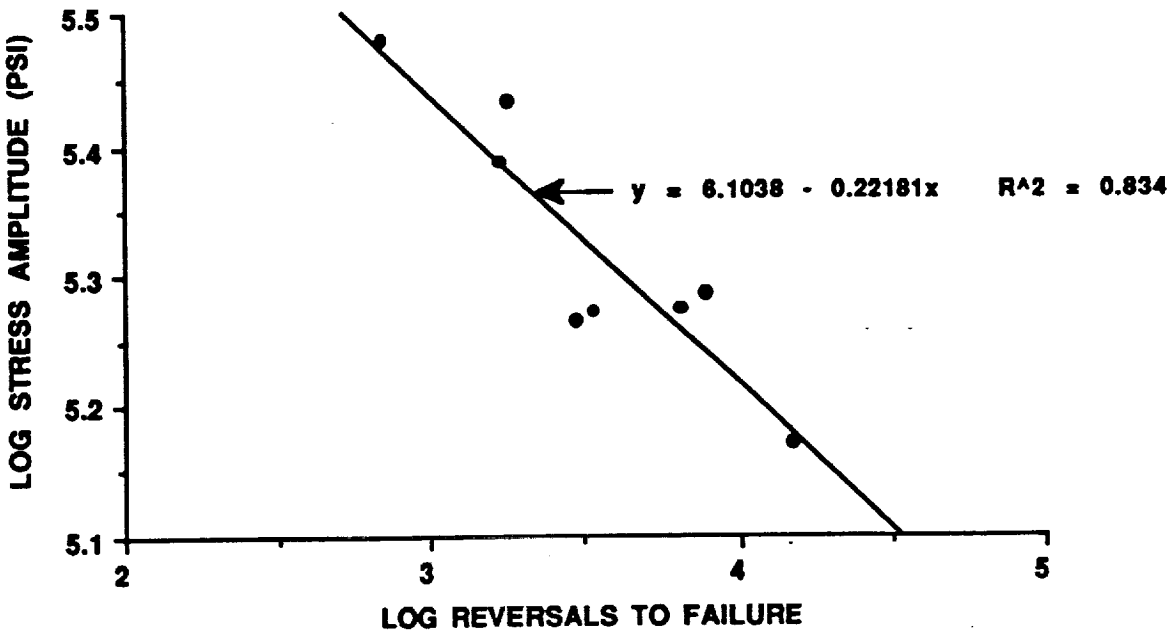

Fig. 7 Regression of Equation (12) Yielding Fatigue Strength Coefficient, σ'_F and Fatigue Strength Exponent, b.

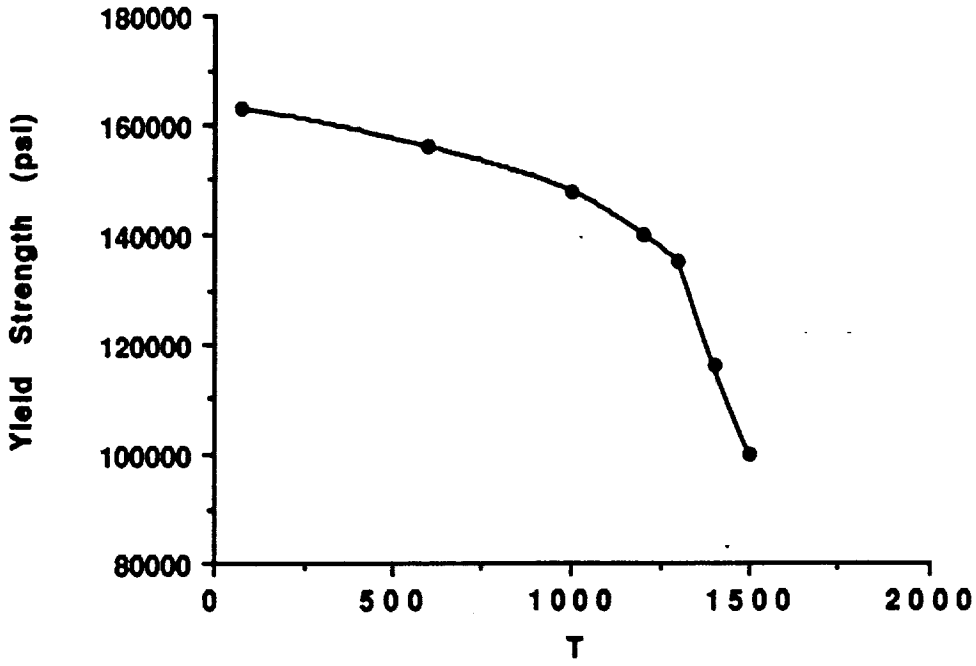

Fig. 8 Effect of Temperature (°F) on Yield Strength for Inconel 718. (Linear Plot)

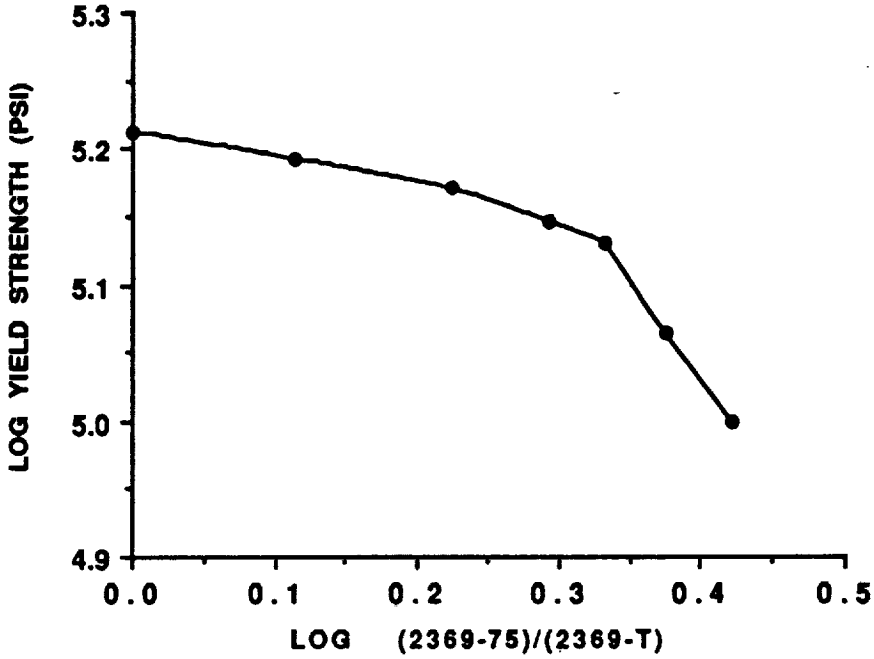

Fig. 9 Effect of Temperature (°F) on Yield Strength for Inconel 718. (Log-Log Plot)

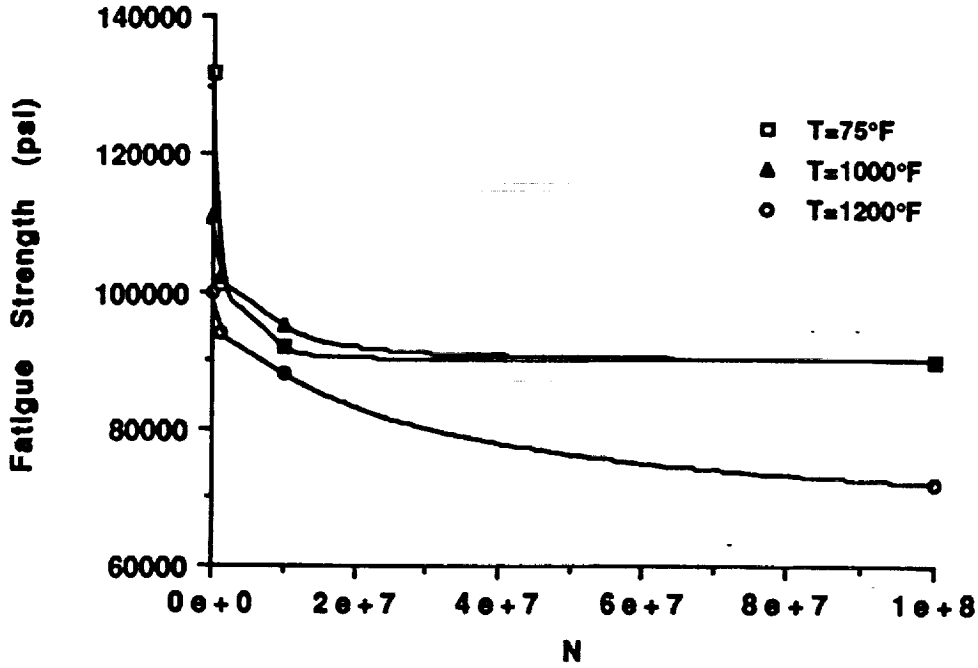

Fig. 10 Effect of Mechanical Fatigue (Cycles) on Fatigue Strength for Inconel 718. (Linear Plot)

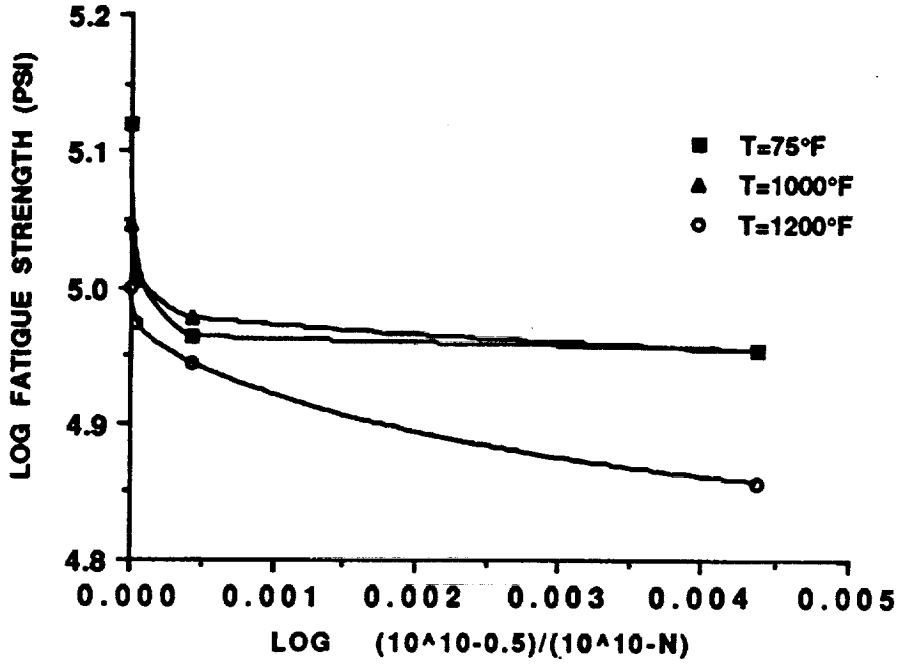

Fig. 11 Effect of Mechanical Fatigue (Cycles) on Fatigue Strength for Inconel 718. (Log-Log Plot)

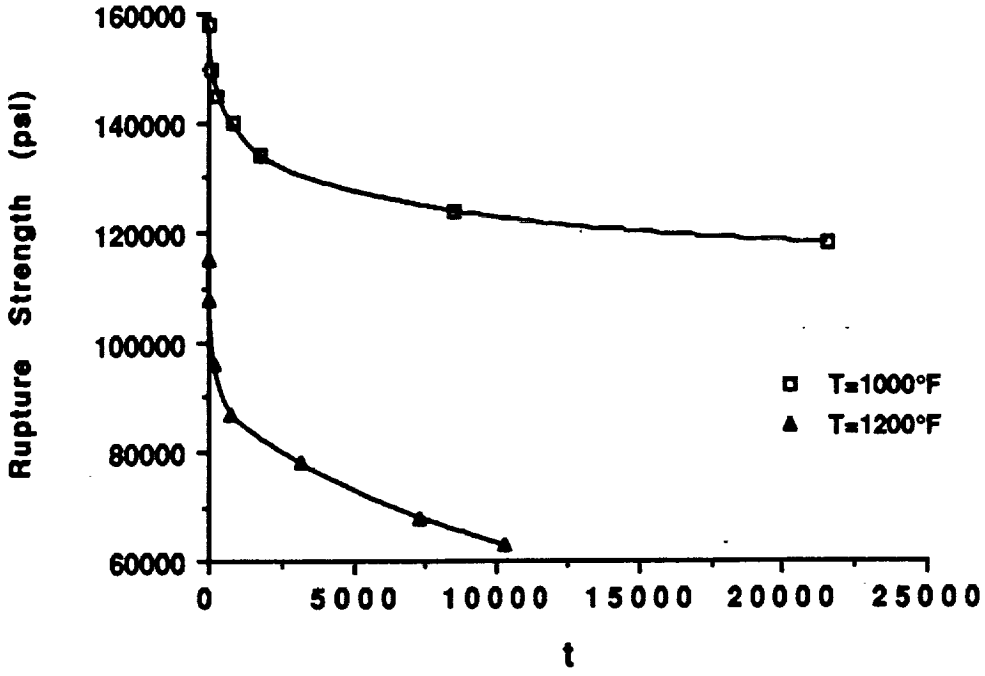

Fig. 12 Effect of Creep Time (Hours) on Rupture Strength for Inconel 718. (Linear Plot)

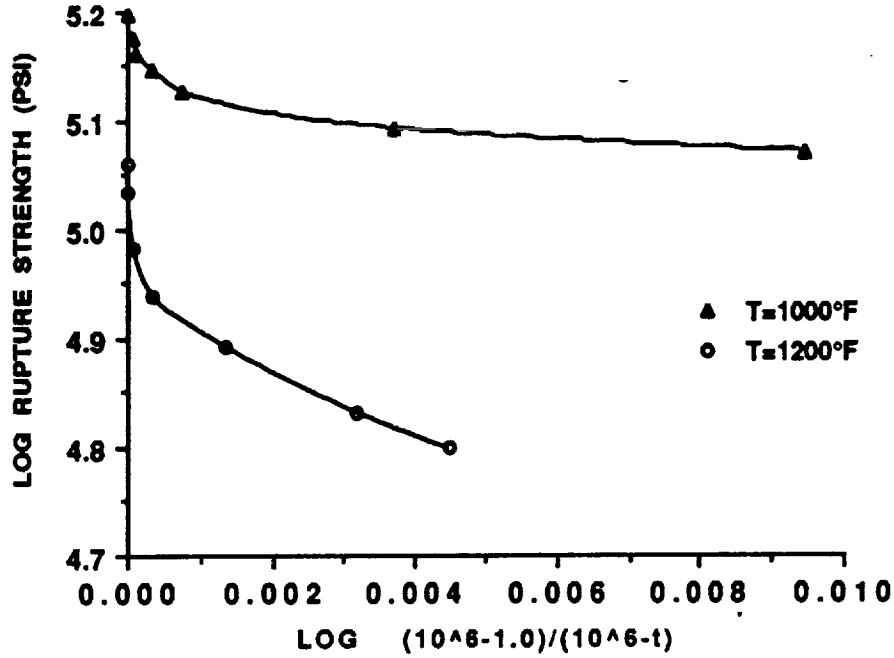

Fig. 13 Effect of Creep Time (Hours) on Rupture Strength for Inconel 718. (Log-Log Plot)

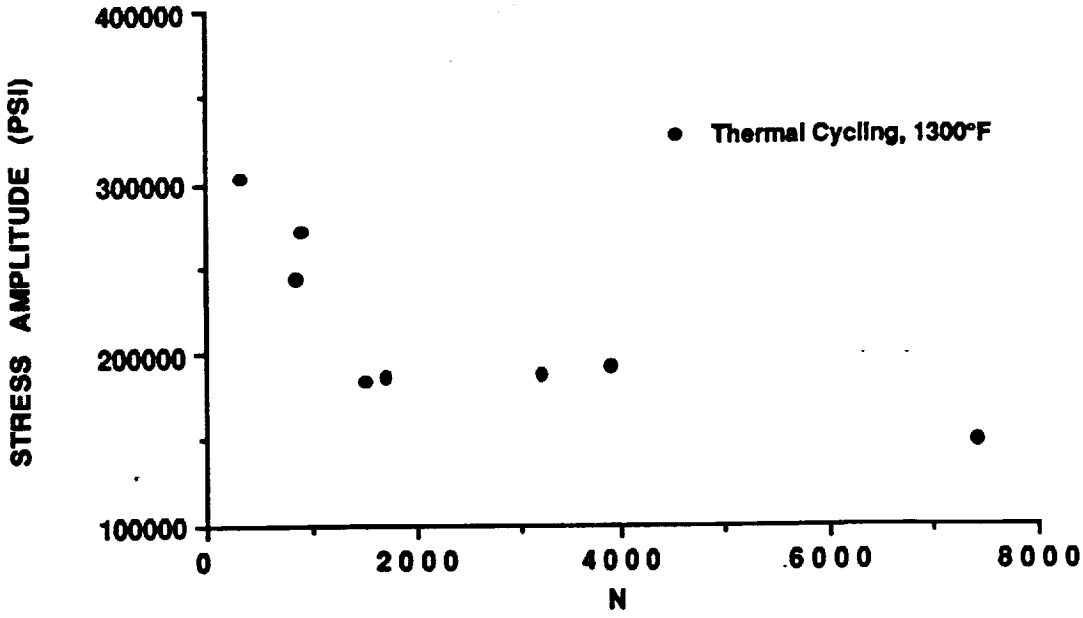

Fig. 14 Effect of Thermal Fatigue (Cycles) on Thermal Fatigue Strength (i.e., Stress Amplitude at Failure) for Inconel 718 (Linear Plot)

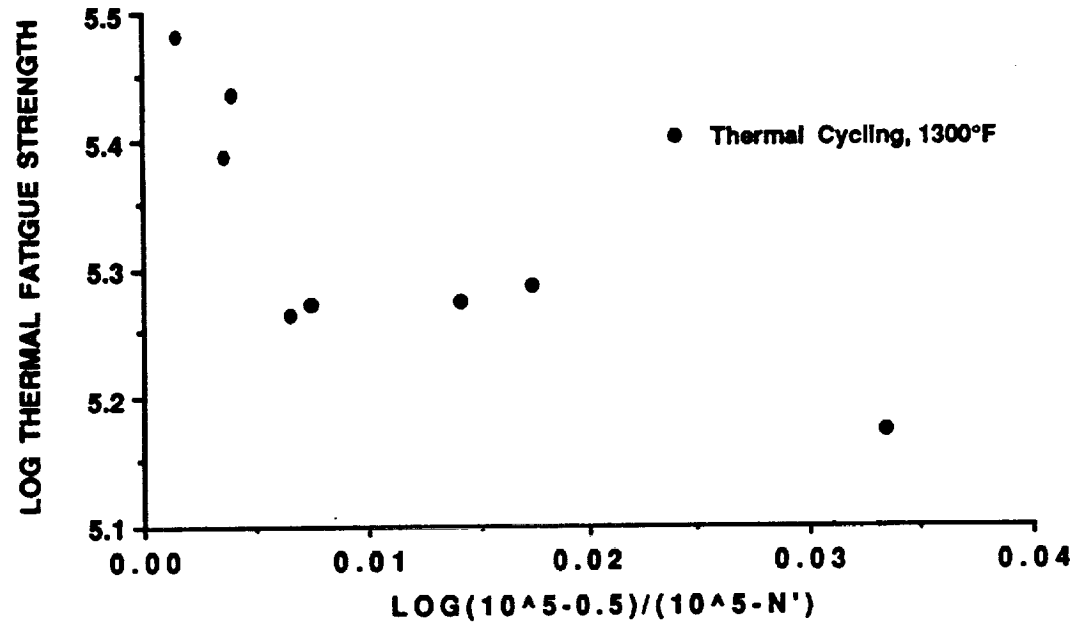

Fig. 15 Effect of Thermal Fatigue (Cycles) on Thermal Fatigue Strength (i.e., Stress Amplitude at Failure) for Inconel 718. (Log-Log Plot)

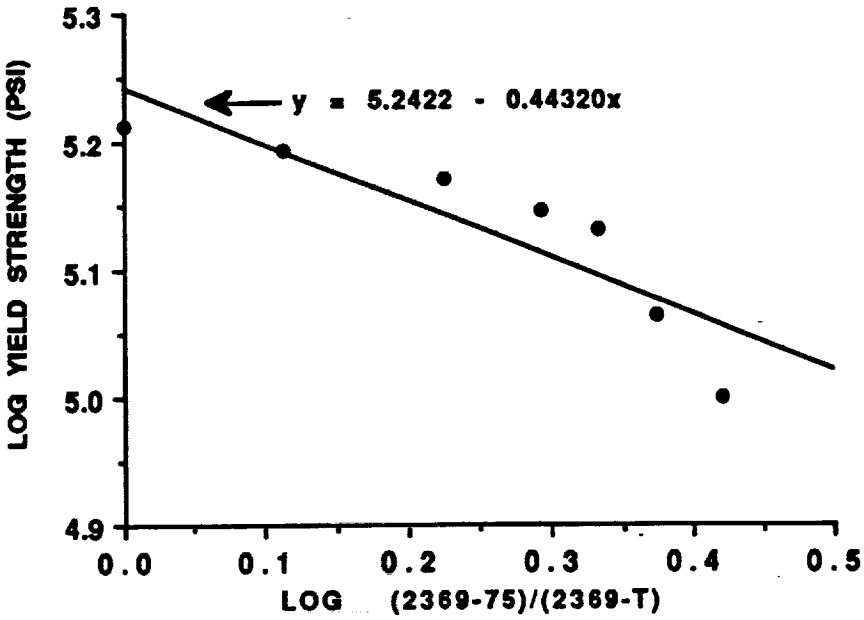

Fig. 16 Effect of Temperature (°F) on Yield Strength for Inconel 718.
(Log-Log Plot with Linear Regression)

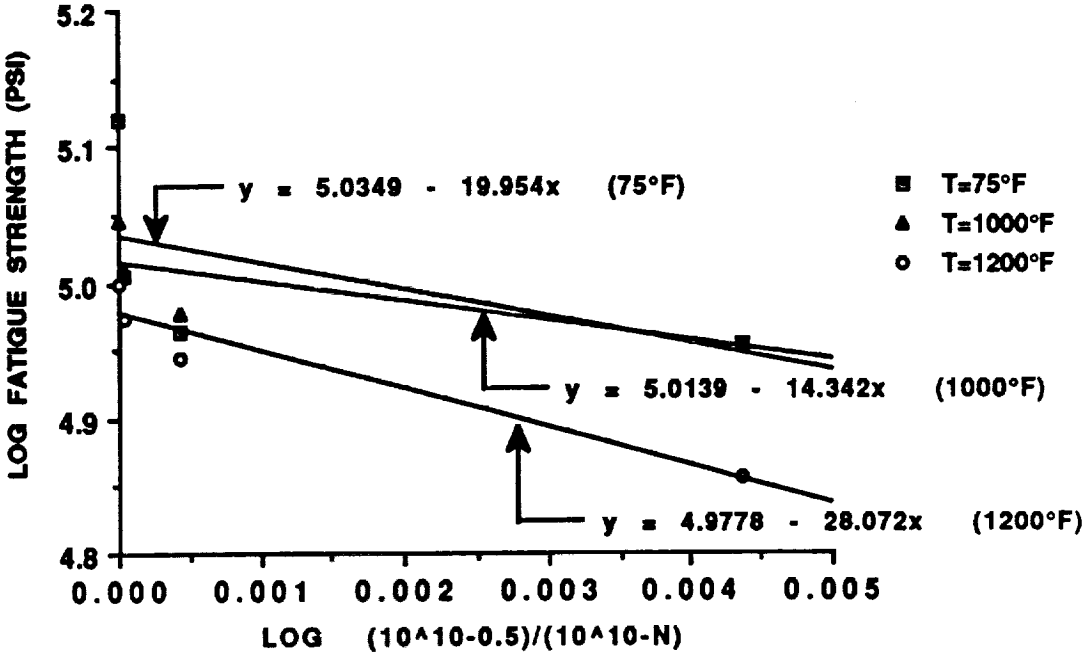

Fig. 17 Effect of Mechanical Fatigue (Cycles) on Fatigue Strength for Inconel 718.
(Log-Log Plot with Linear Regression)

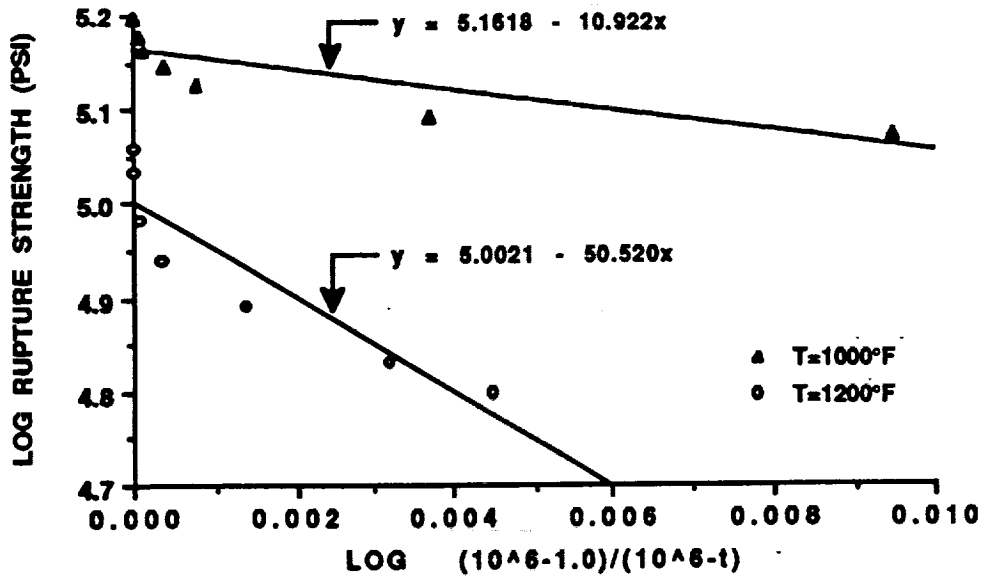

Fig. 18 Effect of Creep Time (Hours) on Rupture Strength for Inconel 718.
(Log-Log Plot with Linear Regression)

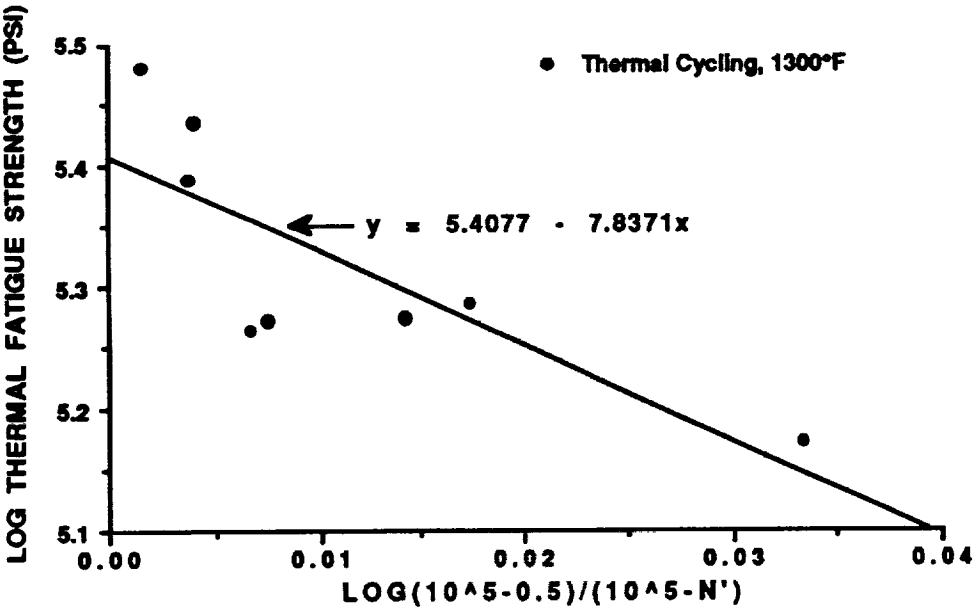

Fig. 19 Effect of Thermal Fatigue (Cycles) on Fatigue Strength for Inconel 781.
(Log-Log Plot with Linear Regression)

7.0 PROBABILISTIC LIFETIME STRENGTH SENSITIVITY STUDY INCLUDING SOME SYNERGISTIC EFFECTS

Using the model given in equation (8), probabilistic lifetime strength was computed using PROMISS. Three effects were included in this study, high temperature, mechanical fatigue and creep. Using the experimental data of Figures 16, 17 and 18 and regression analysis, empirical material constants for these effects, namely, q, s and v were calculated, thus calibrating the model. NASA Lewis Research Center expert opinion and engineering judgment supplied other input values. Typical sets of input values for a PROMISS model represented by equation (8) are given in Tables 6, 7 and 8. For example, Table 6 gives program input data for a current temperature of 75 °F and a current value of mechanical fatigue cycles of 200 (log 200 = 2.3). Note that the creep effect is not applicable (N/A) for low current values of temperature such as 75 °F. The sensitivity study demonstrates the effect of the three variables, high temperature, mechanical fatigue, and creep, on probabilistic lifetime strength. Some of the important input values for this study are given in Table 9. The results of this study, in the form of cumulative distribution functions, are given in Figures 20 to 22, one figure for each effect. For example, Figure 21 shows the effect of mechanical fatigue cycles on lifetime strength. Note that the c.d.f. shifts to the left, indicating a lowering of lifetime strength for increasing mechanical fatigue cycles. In this manner PROMISS results display the sensitivity of lifetime strength to any effect or variable.

The values of the empirical material constants used to calibrate the model and used as input to the PROMISS program are given as mean values in these tables. These constants were calculated individually for each effect, high temperature, mechanical fatigue and creep. Also, inherent in the model given by equation (8) is the assumption that the variables are independent and that there are no synergistic effects.

Table 6 Sensitivity study input to PROMISS for Inconel 718: Temperature = 75 °F.

Effect	Variable Symbol	Units	Distribution Type	Mean	Standard Deviation (Value)	(% of Mean)
Temperature	T_M	°F	Normal	2369.0	71.07	3.0
	T	°F	Normal	75.0	2.25	3.0
	T_O	°F	Normal	75.0	2.25	3.0
	q	N/A	Normal	0.4432	0.01329	3.0
Mechanical Fatigue	N_U	log of cycle	Normal	10.0	1.0	10.0
	N	log of cycle	Normal	2.3	0.35	10.0
	N_O	log of cycle	Normal	- 0.3	- 0.03	10.0
	s	N/A	Normal	19.95	0.5985	3.0
Creep	t_U	hours	Lognormal	N/A	N/A	N/A
	t	hours	Lognormal	N/A	N/A	N/A
	t_O	hours	Lognormal	N/A	N/A	N/A
	v	N/A	Normal	N/A	N/A	N/A

Table 7 Sensitivity study input to PROMISS for Inconel 718: Temperature = 1000 °F.

Effect	Variable Symbol	Units	Distribution Type	Mean	Standard Deviation (Value)	(% of Mean)
Temperature	T_M	°F	Normal	2369.0	71.07	3.0
	T	°F	Normal	1000.0	30.0	3.0
	T_O	°F	Normal	75.0	2.25	3.0
	q	N/A	Normal	0.4432	0.01329	3.0
Mechanical Fatigue	N_U	log of cycle	Normal	10.0	1.0	10.0
	N	log of cycle	Normal	2.3	0.35	10.0
	N_O	log of cycle	Normal	- 0.3	- 0.03	10.0
	s	N/A	Normal	14.34	0.4302	3.0
Creep	t_U	hours	Lognormal	1.0×10^6	5.0×10^4	5.0
	t	hours	Lognormal	100.0	3.0	3.0
	t_O	hours	Lognormal	1.0	0.03	3.0
	v	N/A	Normal	10.92	0.3276	3.0

Table 8 Sensitivity study input to PROMISS for Inconel 718: Temperature = 1200 °F.

Effect	Variable Symbol	Units	Distribution Type	Mean	Standard Deviation (Value)	(% of Mean)
Temperature	T_M	°F	Normal	2369.0	71.07	3.0
	T	°F	Normal	1200.0	36.00	3.0
	T_O	°F	Normal	75.0	2.25	3.0
	q	N/A	Normal	0.4432	0.01329	3.0
Mechanical Fatigue	N_U	log of cycle	Normal	10.0	1.0	10.0
	N	log of cycle	Normal	2.3	0.35	10.0
	N_O	log of cycle	Normal	- 0.3	- 0.03	10.0
	s	N/A	Normal	28.07	0.8421	3.0
Creep	t_U	hours	Lognormal	1.0×10^6	5.0×10^4	5.0
	t	hours	Lognormal	100.0	3.0	3.0
	t_O	hours	Lognormal	1.0	0.03	3.0
	v	N/A	Normal	50.52	1.5156	3.0

Table 9 Sensitivity study of probabilistic material strength degradation model using PROMISS.

Temp. (° F)	Mech. Fatigue (Cycles)	Creep (Hours)
75	200	N/A
1000	200	100
1200	200	100
1000	100	100
1000	200	100
1000	300	100
1000	200	10
1000	200	100
1000	200	190

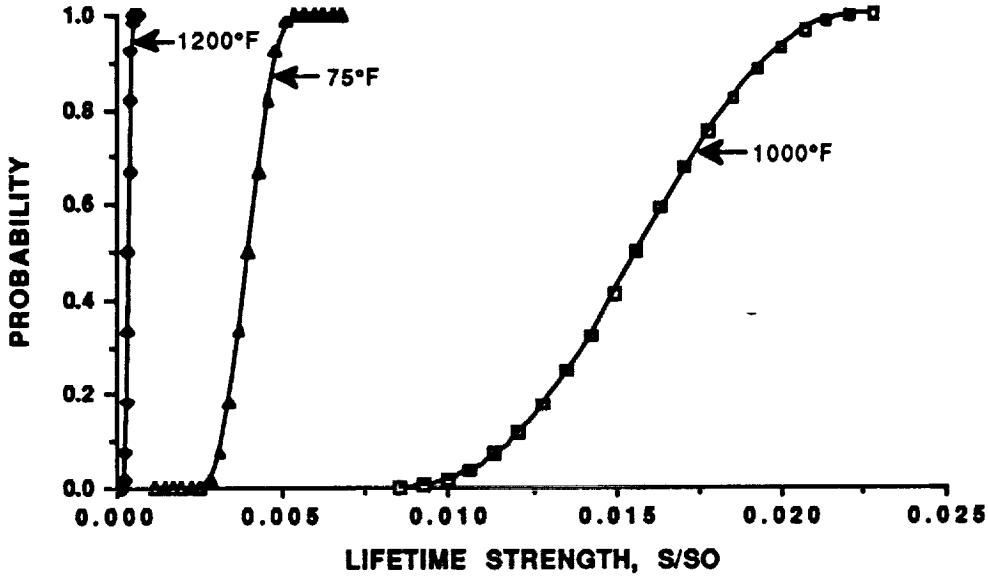

Fig. 20 Comparison of Various Levels of Uncertainty of Temperature (°F) on Probable Strength for Inconel 781 for 200 Cycles of Fatigue and 100 Hours of Creep.

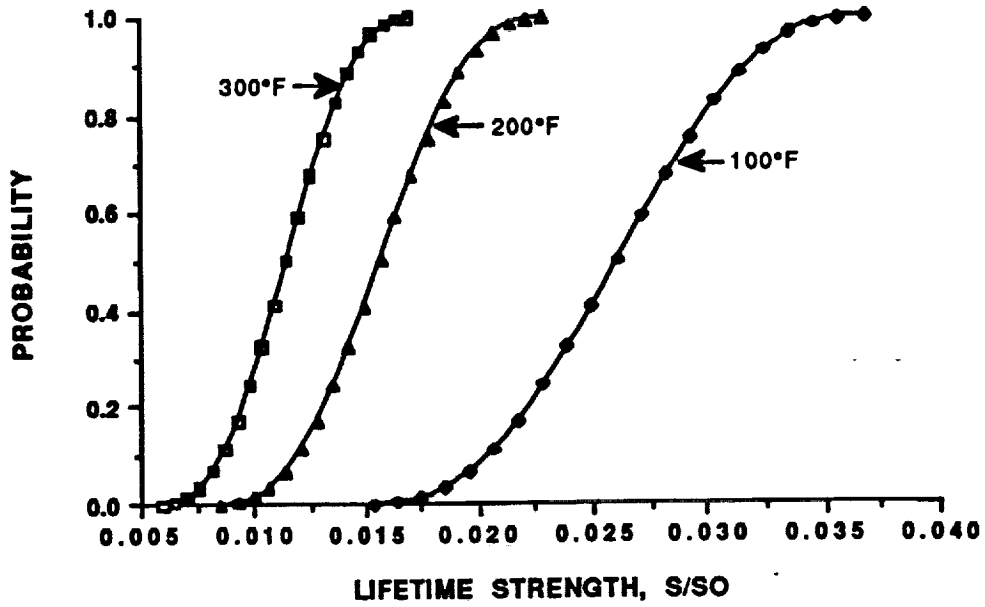

Fig. 21 Comparison of Various Levels of Uncertainty of Mechanical Fatigue (Cycles) on Probable Strength for Inconel 718 for 1000°F and 100 Hours of Creep.

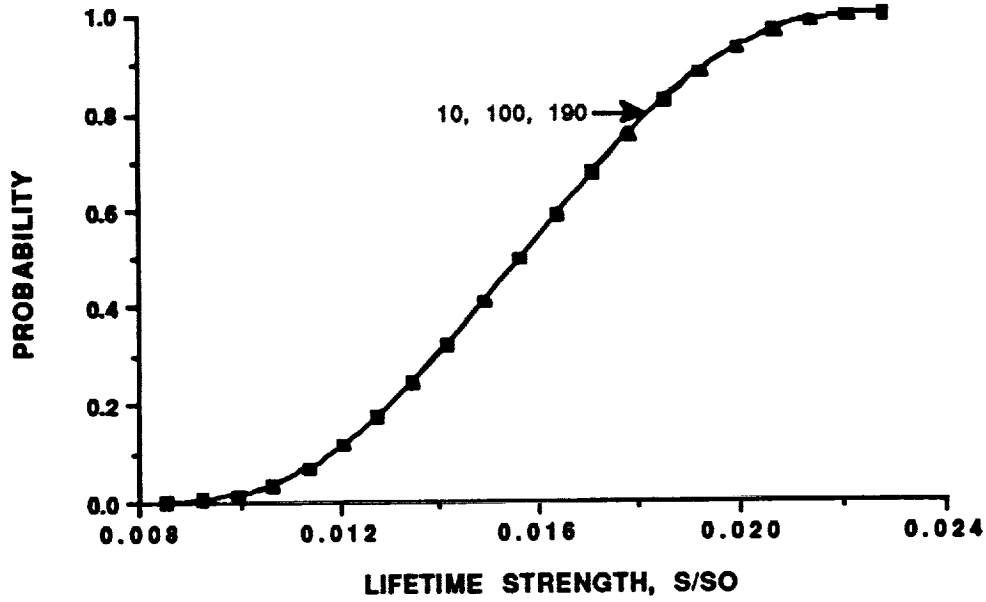

Fig. 22 Comparison of Various Levels of Uncertainty of Creep Time (Hours) on Probable Strength for Inconel 718 for 1000°F and 200 Cycles of Fatigue.

An attempt to take into account synergistic effects included appropriate modifications to input data. For example, it has already been mentioned that creep effects are not applicable at low temperature values. Hence, the input values in Table 6 have been modified such that creep is not applicable at this current temperature. Note also in Tables 6, 7 and 8 that the value of the empirical material constants, s and v, change according to the current temperature value. For example, the creep constant, v, is 10.92 at a temperature of 1000 °F, but increases to 50.52 at 1200 °F. These values of the creep constant are computed from linear regression as shown in Figure 18. The increased value of the constant at 1200 °F is expected. The mechanical fatigue constant, s, also changes as temperature changes. As Figure 17 indicates, however, the data show a lower constant at 1000 °F than at 75 °F. For 1200 °F the constant has definitely increased. These values of the empirical material constant for mechanical fatigue are based upon only four actual test points. Thus for mechanical fatigue, confidence would be increased if a few more actual experimental data points were available.

Simultaneous calibration of the model for all three effects together to build a "combined" or synergistic model to better represent the interdependence of effects may be advantageous. In addition, the subsequent statistical testing of each individual effect, using a synergistic model will assure that it will also model individual effects accurately.

8.0 CONCLUSIONS

A probabilistic material behavior degradation model, applicable to aerospace materials, has been postulated for predicting the random lifetime strength of structural components for aerospace propulsion systems subjected to a number of effects or variables. The model takes the form of a randomized multifactor interaction equation and contains empirical material constants, a_i. Data is available from the open literature for a number of nickel-base superalloys, especially Inconel 718, principally for three individual effects namely, high temperature, mechanical fatigue and creep. Linear regression of this data, together with expert opinion, has resulted in estimates for the empirical material constants through which the model is calibrated. Extension of the model for a fourth effect, thermal fatigue, has been outlined.

Thus, a general computational simulation structure is provided for describing the scatter in lifetime strength in terms of probable values for a number of diverse effects or variables. The sensitivity of random lifetime strength to each variable can be ascertained. Probability statements allow improved judgments to be made regarding the likelihood of lifetime strength and hence structural failure of aerospace propulsion system components.

9.0 ACKNOWLEDGMENTS

The authors gratefully acknowledge the many helpful conversations with Dr. Christos C. Chamis and the support of NASA Lewis Research Center. Also acknowledged are Mr. Paul Van Veen, Undergraduate Research Assistant, of The University of Texas at San Antonio.

10.0 REFERENCES

1. Chamis, C. C., "Simplified Composite Micromechanics Equations for Strength, Fracture Toughness, Impact Resistance and Environmental Effects," NASA TM 83696, Jan. 1984.

2. Hopkins, D. A., "Nonlinear Analysis for High-Temperature Multilayered Fiber Composite Structures," NASA TM 83754, Aug. 1984.

3. Chamis, C. C. and Hopkins, D., "Thermoviscoplastic Nonlinear Constitutive Relationships for Structural Analysis of High Temperature Metal Matrix Composites," NASA TM 87291, Nov. 1985.

4. Hopkins, D. and Chamis, C. C., "A Unique Set of Micromechanics Equations for High Temperature Metal Matrix Composites," NASA TM 87154, Nov. 1985.

5. Boyce, L. and Chamis, C. C., "Probabilistic Constitutive Relationships for Material Strength Degradation Models," Proceedings of the 30th Structures, Structural Dynamics and Materials Conference, Mobile, AL, April 1989, pp. 1832 - 1839.

6. Probabilistic Lifetime Strength of Aerospace Materials Via Computational Simulation by L. Boyce, J. Keating, T. Lovelace, and C. Bast, Final Technical Report, NASA TM 187178, NASA Lewis Research Center, Cleveland, Ohio, Aug. 1991.

7. Computational Simulation of coupled Material Degradation Processes for Probabilistic Lifetime Strength of Aerospace Materials, L. Boyce, C. Bast, Final Technical Report, NASA TM 1887234, NASA Lewis Research Center, Cleveland, Ohio, Mar. 1992.

8. Ross, S. M., Introduction to Probability and Statistics for Engineers and Scientists, Wiley, New York, 1987, p. 278.

9. Siddall, J. N., "A Comparison of Several Methods of Probabilistic Modeling," Proceedings of the Computers in Engineering Conference, ASME, Vol. 4, 1982, pp. 231-238.

10. Scott, D.W., "Nonparametric Probability Density Estimation by Optimization Theoretic Techniques," NASA CR-147763, April 1976.

11. Manson, S.S., Thermal Stress and Low-cycle Fatigue, McGraw-Hill Book Co., N.Y., 1966. p. 256.

12. Swindelman, R. W. and Douglas, D.A., "The Failure of Structural Metals Subjected to Strain-Cycling Conditions," Journal of Basic Engineering, ASME transactions, 81, Series D, 1959, pp. 203 -212.

13. Collins, J. A., Failure of Materials in Mechanical Design, Wiley-Interscience Publication, John Wiley & Sons, N.Y., 1981, pp. 391 - 393.

14. INCONEL 718 Alloy 718, Inco Alloys International, Inc., Huntington, WV, 1986, pp. 8-13.

15. Cullen, T. M. and Freeman, J. W., The Mechanical Properties of INCONEL 718 Sheet Alloy at 800°F 1000°F and 1200°F, NASA CR 268, National Aeronautics and Space Administration, Washington, DC, 1985, pp. 20-34.

16. Barker, J. F., Ross, E.W. and Radavich, J. F., "Long Time Stability of INCONEL 718," Journal of Metals, Jan. 1970, Vol. 22, p. 32.

17. Sims, C. T., Stoloff, N.S. and Hagel, W.C., Superalloys II, Wiley, New York, 1987, pp. 581-585, 590-595.

18. Bannantine, J.A., et. al., Fundamentals of Metal Fatigue Analysis, PrenticeHall, Englewook Cliffs, N.J., 1990, pp. 63 - 66.